Fourier-Transform InfraRed (FTIR) Spectrometry

M.Buschmann, C. Petri, H. Winkler, et al.

Last Change: June 2019

Contents

1 Objectives

- Learn how a Fourier-transform spectrometer works
- Investigate the relation between absorbance and concentration of water vapour
- Investigate the absorption cross section of H_2O
- Investigate the atmospheric black body emission temperature

2 Fundamentals

2.1 Fourier-transform spectrometry

2.1.1 Principles of a Fourier-transform spectrometer

A Fourier transform spectrometer (FTS) is in principle a Michelson interferometer. The basic components of a FTS are pictured in Figure 1. The incident radiation is divided into two optical paths by a beam splitter. Ideally 50 % are reflected onto a fixed mirror and 50 % transmitted onto a moveable mirror. Both beams are reflected by the mirrors where they then recombine at the beamsplitter and interfere. 50 % of the recombined beam is directed back to the entrance of the spectrometer, and 50 % is directed to the detector, where the interference is recorded and converted into a digital signal. By shifting the moveable mirror, the dependency of the interference on the optical path difference (OPD) is recorded. The interference is called an interferogram and the spectrum of the incident radiation is calculated with a Fourier transformation from the interferogram. A Fourier-transform (FT) of a function $f(x)$ and the inverse Fourier-transform FT^{-1} are defined as

$$\mathrm{FT}(f(x)) = F(y) = \int_{-\infty}^{\infty} f(x) e^{i2\pi xy} dx \tag{1}$$

$$\mathrm{FT}^{-1}(F(y)) = f(x) = \frac{1}{2\pi} \int_{-\infty}^{\infty} F(y) e^{-i2\pi xy} dy \tag{2}$$

With Euler's formula, $e^{2\pi xy}$ is written as $\cos(2\pi xy) + i\sin(2\pi xy)$. The integral of an even function $f(x)$ multiplied with a sine wave is zero and for an even function, Equation 1 becomes

$$F(y) = \int_{-\infty}^{\infty} f(x) \cos(2\pi xy) dx \tag{3}$$

The interference, recorded by the detector of a FTS, can be expressed as $F(y)$ in Equation 3, and the inverse Fourier transform $f(x)$ is the spectrum of the incident radiation, as shown in the following. The incident radiation can be described as a plane wave E_{inc} with amplitude $\mathrm{E}_{0,inc}$ which is in case of monochromatic radiation modulated by a harmonic function, $e^{i(kx-\omega t)}$, with the wave vector, k, the angular frequency, ω, the position vector, x, and the time, t.

$$E_{inc}(k,t) = E_{0,inc} e^{i(kx-\omega t)} \tag{4}$$

The superposition of the interfering beams can be described by the superposition of two plane waves with the same frequency

$$\begin{aligned} E &= E_1 + E_2 = E_0 e^{i(kx_1-\omega t)} + e^{i(kx_2-\omega t)} \\ &= E_0 e^{-i\omega t} e^{ikx_1} + e^{ikx_2} \end{aligned} \tag{5}$$

The intensity of the detected superposition, $I = |E|^2$, is then given by

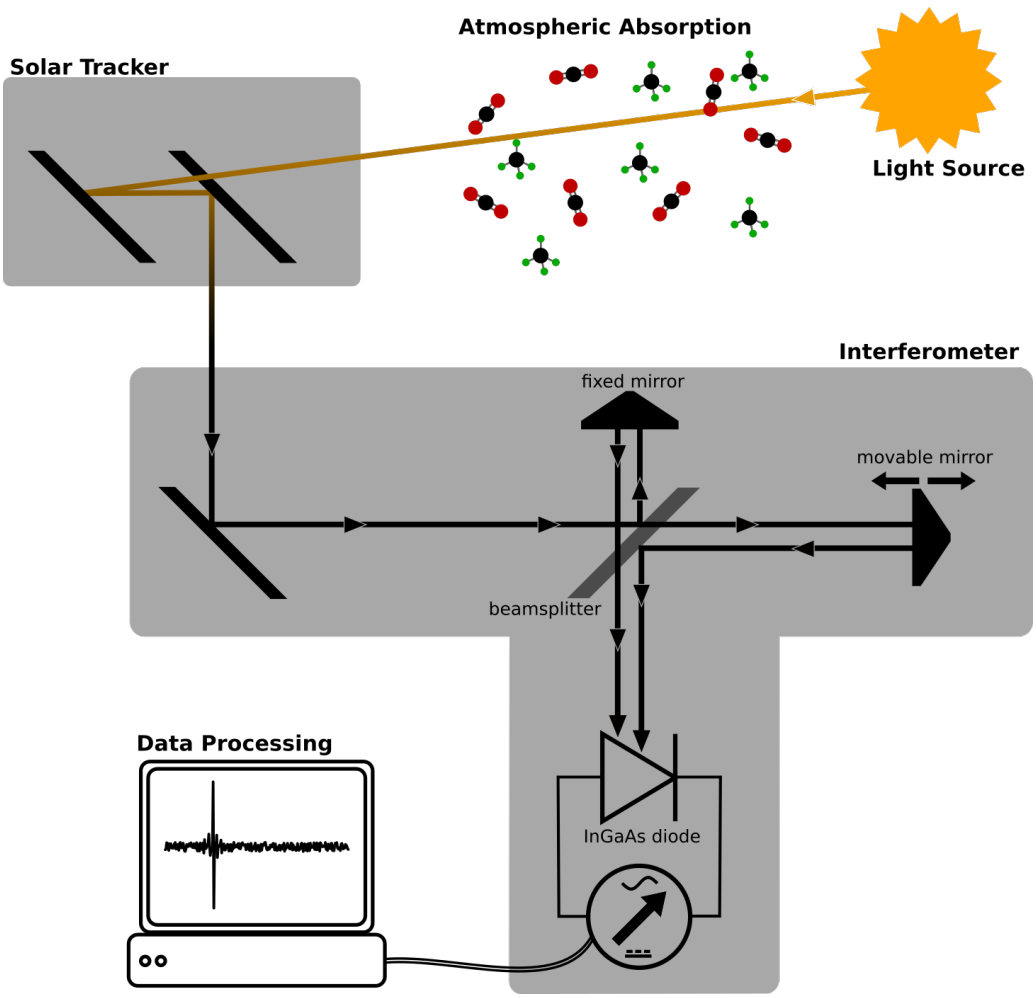

Figure 1: A Fourier-transform spectrometer (in absorption geometry) with its principle components. The beam from the light source is separated by a beam splitter into two beams. Both beams are reflected by mirrors and the interference is recorded at a detector. By moving one mirror, the optical path difference (OPD) is varied. The resulting interference pattern, the interferogram, is recorded. The spectrum of the incident light source is calculated from the interferogram via a Fourier-transform.

$$
\begin{aligned}
I &= E_0^2 \left(e^{ikx_1} + e^{ikx_2} \right) \\
&= E_0^2 \left(1 + 1 + e^{ik(x_1 - x_2)} + e^{-ik(x_1 - x_2)} \right) \\
&= 2E_0^2 \left(1 + \cos(k(x_1 - x_2)) \right)
\end{aligned} \tag{6}
$$

With the optical path difference $x = (x_1 - x_2)$, $B(\nu) = 2E_0^2$ as the spectral energy and $\nu = \frac{k}{2\pi}$, the equation becomes

$$
I(x) = B(\nu)(1 + \cos(2\pi\nu x)) \tag{7}
$$

In the case of a monochromatic light source, e.g. a laser, the signal at the detector is therefore described by a a cosine function; in the case of polychromatic light sources, e.g. the continuous spectrum of the sun, the signal at the detector will be a superposition of the contributions of all the different frequencies.

$$
I(x) = \int_0^\infty B(\nu)(1 + \cos(2\pi\nu x))d\nu \tag{8}
$$

The interferogram (Equation 8) is the sum of a constant term, $B(\nu)$, the DC term, and a varying term, $B(\nu)\cos(2\pi\nu x)$, the AC term. The DC term is the intensity of the incident radiation, and the AC term contains all information about the spectral structure. Under the assumption of a constant intensity of the incident radiation, only the AC term was recorded until recently in atmospheric research. The spectrometers can now record the DC term because of technical improvements and one can now correct for intensity fluctuations due to e.g. passing clouds. The extension to $-\infty$ of the integral in Equation 8 allows a Fourier-transform of the recorded AC term of the interferogram (A factor of $(2\pi) - 1$ is omitted in the following).

$$
\begin{aligned}
I(x) &= \int_{-\infty}^{\infty} B'(\nu)\cos(2\pi\nu x)d\nu \\
B'(\nu) &= \int_{-\infty}^{\infty} I(x)\cos(2\pi\nu x)dx
\end{aligned} \tag{9}
$$

The Fourier-transform of an even function $f(x)$ produces two equal Fourier-transforms $F(y)$ and $F(-y)$, because of $cos(2\pi x) = cos(-2\pi x)$. The Fourier-transform of an interferogram therefore produces a physical spectrum $B(\nu)$ and an *un*physical spectrum $B(-\nu)$ at negative frequencies. For complete symmetry in the transform, an even spectrum $B_e(\nu)$ is constructed:

$$
B_e(\nu) = \frac{1}{2}\left(B(\nu) + B(-\nu)\right) = \int_{-\infty}^{\infty} I(x)\cos(2\pi\nu x)dx \tag{10}
$$

With this equation the spectrum of the incident radiation $B(\nu)$ can be calculated. In the next chapter the usage of Fourier-transform spectrometry for solar absorption measurements will be introduced.

2.1.2 Solar absorption FTS measurements

Fourier-transform spectrometry (FTS) is used in atmospheric physics as a passive remote sensing method that is widely applicable. Example use cases are ground-based FTS instruments [Notholt and Schrems, 1994; Wunch et al., 2011] and instruments on balloon flights or satellites, like MkIV [Toon, 1991], MIPAS [Fischer et al., 2008], ACE-FTS [Foucher et al., 2011], GOSAT [Morino et al., 2011]. Solar absorption Fourier-transform spectrometry uses the sun as a light source. The sun beam is directed into the FTS with a solar tracker, which follows the position of the sun throughout the day. Atmospheric gases absorb solar radiation. The high energetic UV radiation is absorbed by the outer layer of the atmosphere due to absorption of O_2 and and O_3. The visible radiation is mostly scattered by molecules and aerosols and reaches the lower layers of the atmosphere.

type of gas	gases
constant	O_2, N_2
long-lived	CO_2, N_2O, CH_4, CFC-11
tropospheric	C_2H_2, C_2H_6, CH_2O, CO, HCN, CO_2, SF_6, NH_3, H_2O
stratospheric	O_3, HCl, ClO, $ClONO_3$, HNO_3, NO_2, NO, COF_2

Table 1: The FTS is used for analyses of various gases. Some are listed here. The gases are grouped as constant, long-lived, and their main occurrence in the troposphere or stratosphere.

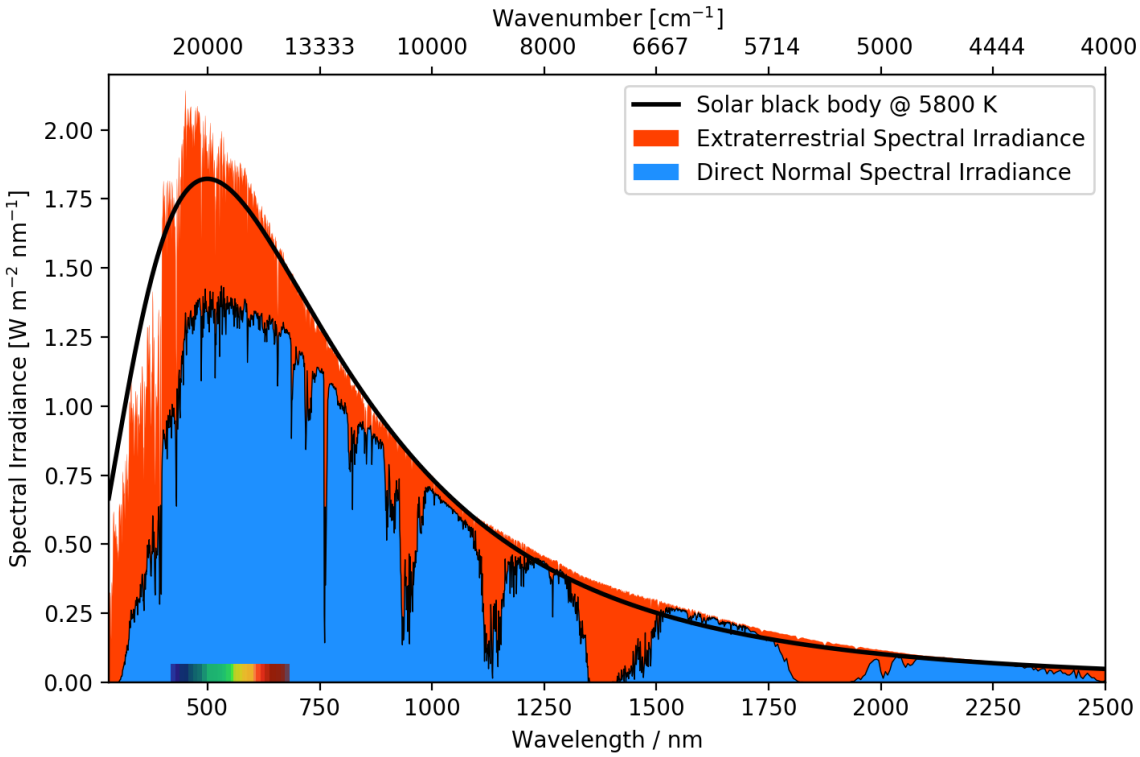

Figure 2: A solar radiation spectrum at the top of atmosphere and on the Earth's surface. Source of irradiance data: http://rredc.nrel.gov/solar/spectra/am1.5/

Various molecules absorb in the infrared spectral region, a large part is absorbed by H_2O, CH_4 and CO_2. Therefore the solar spectrum at the top of the atmosphere is different to the radiation that is measured at the Earth's surface (see Figure 2). The absorption lines measured by the FTS are assigned to atmospheric molecules, as they absorb only discrete and specific frequencies according to their molecular energy levels. The atmospheric concentrations of the interfering gases are retrieved by comparing measured transmission spectra with simulated transmissions based on measurements in laboratories, e.g. HITRAN database [Rothman and Young, 1981]. Some basics introduction on the origin of absorption lines in the near infrared are described in Section 2.3.
Technically, a broad range of the solar spectrum can be measured with a FTS instrument, given the appropriate selection of detectors and beam splitter. The most important gases are listed in Table 1.

2.2 Absorption coefficient, absorbance, cross-section

The absorption of electromagnetic radiation passing through a medium is described by the Lambert-Beer law. For a infinitesimally thin layer with height ds, the change of the intensity $I(\nu)$ is given by:

$$\frac{dI(\nu)}{ds} = -\alpha(\nu)I(\nu) \tag{11}$$

with the absorption coeffcient α (in units of 1/length). For a homogeneous medium, integration of 11 along the path of the ray gives

$$I(\nu) = I_0(\nu)e^(- \alpha(\nu)s) \tag{12}$$

where $\tau(\nu) = \alpha(\nu)s$ is the optical thickness or optical path. In spectroscopy, the absorbance A can be defined as:

$$A(\nu) = log_{10}(I_0(\nu)/I(\nu)) \tag{13}$$

(or sometimes with $ln(...)$ instead of log_10). The absorption coefficient $\alpha(\nu)$ of a medium is proportional to the number of absorbers (here: molecules) and their absorption strength:

$$\alpha(\nu) = \sigma(\nu)\frac{N}{V} \tag{14}$$

with the absorption cross section σ (in units of an area), and $\frac{N}{V}$ the number density of the absorbers (here: molecules per unit volume).

2.3 Relevant basics of molecular physics

The energy, a molecule absorbs or emits, is not continuous, as molecular energy states are discrete and only radiation with a wavelength corresponding to the energy gaps can be absorbed or emitted. The molecular spectra are called band spectra and contain electron transitions, rotational-vibrational transitions and pure rotational transitions:

$$\begin{aligned} T &= T^{el} + G^{vib}_{\nu} + F^{rot}_{\nu,J} \\ &= \frac{E_{el}}{hc} + \frac{\hbar\omega}{hc}(\nu + \frac{1}{2}) + B \cdot J(J+1) \end{aligned} \tag{15}$$

with the vibrational quantum number $\nu(= 0, 1, 2, \dots)$ and the rotational quantum number $J(= 0, 1, 2, 3, \dots)$. $B = \frac{h}{8\pi^2 c\theta}$ is the rotational constant of the molecule (θ: moment of inertia) [Haken and Wolf, 2013].

In order to calculate possible absorptions due to rotational-vibrational and electronic transitions separately, the Born-Oppenheimer approximation is useful. It assumes that due to the much higher mass of the nuclei compared to the mass of the electrons, the movement of the nuclei are negligible compared to the electrons, and a static potential can be assumed for the electrons. The physically accurate absorption lines are results of quantum mechanical transition matrix elements, which will not be described in this introduction. The physical process can, nevertheless, be understood in a semi-classical approach. A semi-classical approach means that classic concepts, like the orbital angular momentum, are used with a subsequent quantization.

Pure rotational transitions are observed in the microwave region, if the molecule has a permanent electric dipole moment. Vibrational transitions are mostly accompanied by rotational transitions and result in combined rotational-vibrational transitions in the infrared region and will be discussed in more detail.

Vibrational transitions can be described by the harmonic oscillator concept underlying the second term of Equation 15. For the harmonic oscillator, only transitions with $\Delta\nu = \pm 1$ are allowed. The real potential is not symmetric as at nearer distances to the nucleus repulsive forces increase and at larger distances dissociation occurs. This anharmonic oscillator is approximated by a Morse potential and leads to so called overtone bands with $\Delta\nu = \pm 2, \pm 3, \pm 4, \dots$ with quickly decreasing intensities.

Rotational transitions can be described by the quantum mechanical selection rule $\Delta J = \pm 1$ (see Equation 15). Transition with $\Delta J = -1$ lead in a rotational-vibrational spectrum to lower wave numbers as the vibrational transition frequency, called the P-branch. Towards higher wave numbers, lines of transition with $\Delta J = +1$, called the R-branch, are found.

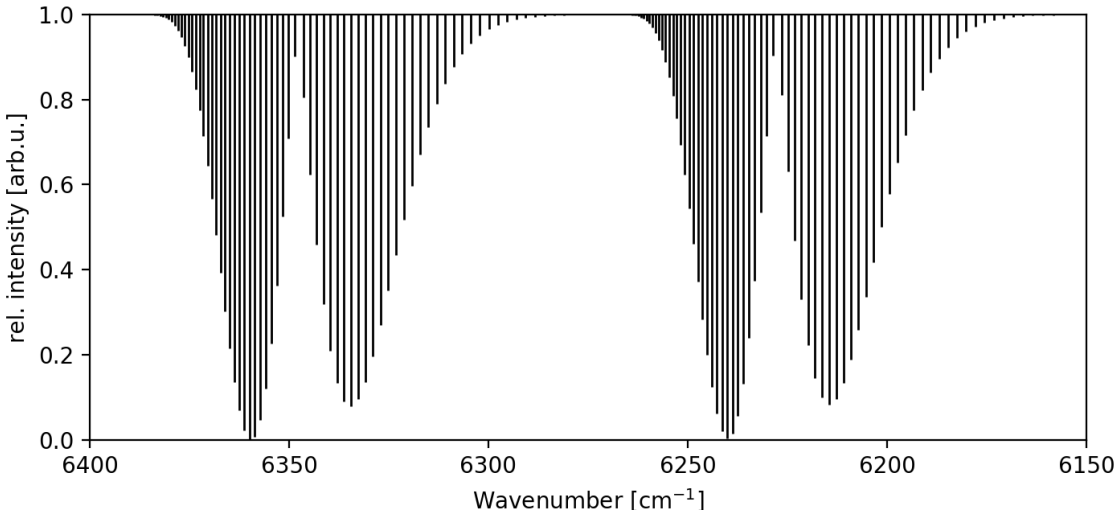

Figure 3: CO_2 absorption line positions and intensities around 6220 cm^{-1} and 6339 cm^{-1}, which are often used for analysis in atmospheric science. Line parameters from http://www.cfa.harvard.edu/HITRAN/

The existence of the Q-branch, the vibrational transition frequency without rotational transition ($\Delta J = 0$) is dependent on the symmetry of the molecular structure. As an example for rotational-vibrational transitions, CO_2 transition bands, analysed in atmospheric science, are pictured in Figure . The bands are due to transitions of combinations of the fundamental vibrational modes. The linear CO_2 molecule has four fundamental vibrational modes (degrees of freedom $f = 3N - 5 = 4$ with N: number of mass points): $\nu_1 = 1337$ cm^{-1} , $\nu_2 = 667$ cm^{-1} (two-fold degeneracy), $\nu_3 = 2349$ cm^{-1}. ν_1 is the symmetric stretching, ν_2 the bending and ν_3 the antisymmetric stretching vibration mode of the CO_2 molecule.
For example, the transition band centered around $\nu = 6228$ cm^{-1}, often used in atmospheric remote sensing of carbon dioxide originates in a combination of the fundamental vibrational modes: $1\nu_1$, $4\nu_2$, and $1\nu_3$. In spectroscopic notation this is denoted as the transotion $(1\,4^0\,1) \rightarrow 0\,0^0\,0$, the ground state. The shape of the P- and R-branches is determined mostly by the degeneration $2J + 1$. For higher J (Equation 15 with $J = 0, 1, 2, 3, \dots$) the degeneration, and therefore the line intensity, increases. Secondly, the population density of the molecular energy levels is governed by the Boltzmann distribution (in thermodynamic equilibrium). Energy levels with higher J are less populated at a given temperature. These two processes lead to the shape of the branches. With the population densities of two levels, n_1 and n_2 and the degeneration, g_1 and g_2 of these levels, the population probability is given by the Boltzmann distribution (in thermodynamic equilibrium) Haken and Wolf [2013]:

$$\frac{n_1}{n_2} = \frac{g_1}{g_2} e^{\frac{-(E_1 - E_2)}{k_B T}} = g_1 e^{\frac{-hcBJ(J+1)}{k_B T}} \tag{16}$$

The overall asymmetric levels of the P- and R-branch result from the higher population number in the lower energy levels. From the equidistant gaps of the rotational transitions, the rotational constant B can be calculated according to the third term of Equation 15. The rotational constant B includes information about the molecule's properties, like the nuclei distance. Deviations in the spacings are due to the fact that the underlying assumption of the molecule as a rigid rotor is just an approximation. Especially for higher values of J, the effective distance between the nuclei increases, as well as the momentum of inertia. As the spacing is proportional to the rotational constant B, which is inversely proportional to the momentum of inertia, the spacing reduces towards higher values of J, similarly the flanks of the line. This is observed in pure rotational spectra in the microwave region as well. In the near infrared region, this relationship is amplified due to the coupling of the vibrational and rotational movement: As a molecule vibrates ≈ 1000 times in one rotation, the effective internuclear distance increases.

In **Electron transitions**, the energy of one electron is a result of the distance to the almost static atomic nuclei and the electron configuration of the other electrons in the molecule. The transition between two electronic states are ruled by the Franck-Condon principle, which states that an electronic transition occurs without changes in the nucleus positions during a transition, as the electronic transitions occur in times of about 10^{-15} seconds. The most probable electronic transition happens for two vibrational energy levels, whose vibrational wave functions overlap significantly.

2.4 Total Power Method

The spectral power that is received by the spectrometer is composed of two parts: the actual spectrum and the system noise. The actual spectrum is superimposed together with the system noise of the instrument. The spectral power P_a of the atmosphere can be expressed in terms of brightness temperatures, which is proportional to the spectral power:

$$P_a = G(T_{B,a} + T_{B,sys}) \tag{17}$$

where $T_{B,a}$ is the measured signal from the atmosphere, G is an amplifying factor and $T_{B,sys}$ is the system noise temperature. The system noise is present even if no radiation is measured. It originates from several sources, e.g. from thermal noise in the amplifiers.
The method depends on a sufficiently strong spectral signature. All three variable in Equation 17 are unknown. Two additional relations are needed. They are taken from measuring a hot and a cold black body (using the black body radiator):

$$P_h = G(T_{B,h} + T_{B,sys}) \tag{18}$$
$$P_c = G(T_{B,c} + T_{B,sys}) \tag{19}$$

where P_h is the spectra power from the hot black body and P_c is the spectral power from the cold black body. The radiation $T_{B,h}$ and $T_{B,c}$ of the black bodies is well known when we know their physical temperatures. Using equations 17, 18 and 19, we obtain an expression for the atmospheric signal utilizing spectra from a hot and cold black body and spectra from the atmosphere:

$$T_{B,a} = T_{B,c} + \frac{T_{B,h} - T_{B,c}}{P_h - P_c}(P_a - P_c) \tag{20}$$

3 Experiments

3.1 Part I: Absorption of gases within the laboratory

In this part, the water vapour in the laboratory air is analysed by recording absorption spectra while the relative humidity in the room is changed. From the absorption lines, the H_2O absorption cross-section is calculated.

3.1.1 Experimental setup

1. Record environmental and meta data like temperature, relative humidity, pressure and the names of the measured spectra for all experiments, and every time a spectrum is recorded.

2. Fill both detectors with liquid Nitrogen (LN_2) and fill the water heater with about a litre of water.

3. Set the black body radiator temperature to 125°C and place it in front of the entrance of the FTS. Measure the background signal R(ν) with the experiment file *lki1000_prac.XPM* after aligning for signal maximum.

4. Measure the sample spectra S(ν), by positioning the black body source on the next floor after aligning for signal maximum. Perform the measurement at least 5 times, each time with different relative humidity in the room (no change, boiling water (3x), after opening the windows).

5. Save the recorded spectra as ASCII-text files. The files will be sent to you at the end of the day.

3.1.2 Analysis and report preparation

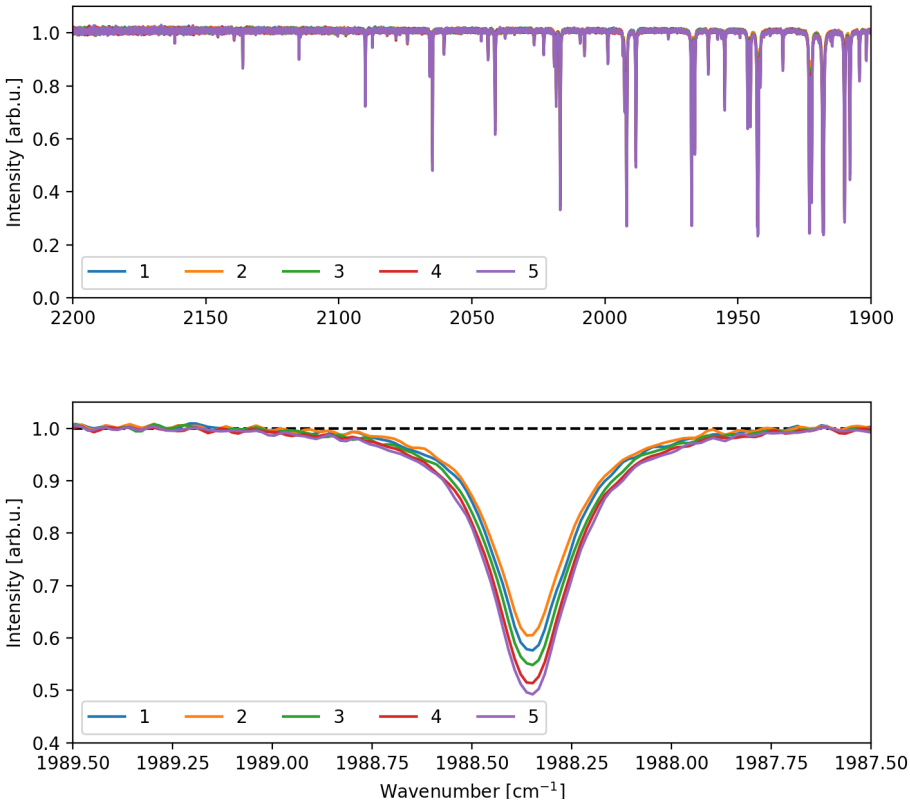

Figure 4: Top: The calculated transmission spectra recorded in the lab. Bottom: Zoom to one example H_2O absorption line recorded under different environmental conditions (changing relative humidity).

1. From the sample and background spectra (S(ν) and R(ν)), calculate the transmission spectra $T(\nu)$ (see top panel in Figure 4) via

$$T(\nu) = \frac{S(\nu)}{R(\nu)} \tag{21}$$

2. The absorbance A, can be determined by zooming into a specific H_2O absorption line (see bottom panel in Figure 4). Choose 3 different H_2O absorption lines and calculate the corresponding absorbances:

$$A_{min} = -log_{10}(T_{max}) \tag{22}$$
$$A_{max} = -log_{10}(T_{min}) \tag{23}$$
$$A = A_{max} - A_{min} \tag{24}$$

3. Validation of results using temperature and relative humidity measurements. The absorbance of water vapour is directly proportional to its concentration:

$$A \propto c_{mol} \tag{25}$$

The concentration of water vapour can be calculated using the recorded temperature and relative humidity measurements via [Alduchov and Eskridge, 1996]:

$$c_{mol} = \theta \frac{6.1094\, e^{\frac{17.625\, T}{T+243.04}}}{R(T+273.15)}\, N_A\, 10^{-6} \tag{26}$$

where $R = 8.3145 Jmol^{-1}K^{-1}$ is the universal gas constant, $N_A = 6.022\, 10^{23} mol^{-1}$ the Avogadro constant, θ the measured relative humidity in the lab

4. For each selection of an absorption line, plot the absorbance A as function of c_{mol} for all recorded trials and fit a line (with 0 intercept) through the data. Determine the slope and the correlation coefficient.

   Answer following questions:

   - What does the slope physically represent?
   - What does the correlation coefficient represent?
   - What might be the main error sources? Estimate the uncertainty.

5. Calculate the absorption cross-section for the considered absorption lines. One needs to know the absorption path length. Here, there are 220 cm between the two positions of the black body radiator (between reference and sample geometry).

3.2 Part II: Atmospheric emissions

Radiation emission from molecules occurs when there is a transition from a higher energy state to a lower energy state. In this experiment, we investigate the atmospheric temperature. We calibrate an atmospheric emission spectrum using a black body radiator emitting at $125°C$ and at $30°C$ using the total power method described previously.

3.2.1 Experimental setup

1. Record environmental and meta data like temperature, relative humidity, pressure and the names of the measured spectra for all experiments.

2. Position the black body radiator on the edge inside the dome and set it's temperature to 125°C. Point the solar tracker to the active surface and note the geo position after optimizing for signal maximum. Record the spectrum P_h by using the experiment file *lkm1000_prac.XPM*. Then set the black body temperature to 30°C. Be careful not to move it.

3. Point the solar tracker into the sky, but not towards the sun. Measure the atmospheric emission spectrum (P_a).

4. After the black body radiator reached it's target temperature of 30°C, record the spectrum P_c after repositioning of the solar tracker to the previously noted geo position.

5. Save the recorded spectra as ASCII-text files. The files will be sent to you at the end of the day.

3.2.2 Analysis and report preparation

1. Check the obtained spectra P_c and P_a for the correct phase correction. If wrong, re-apply the phase correction with the phase of P_h.

2. Determine the atmospheric emission $T_{B,a}$ by using the total power method presented in Section 2.4

3. Briefly discuss the meaning and origin of the calculated temperature value.

References

Oleg A. Alduchov and Robert E. Eskridge. Improved magnus form approximation of saturation vapor pressure. *Journal of Applied Meteorology*, 35(4):601–609, 1996. doi: 10.1175/1520-0450(1996)035⟨0601:IMFAOS⟩2.0.CO;2. URL https://doi.org/10.1175/1520-0450(1996)035<0601:IMFAOS>2.0.CO;2.

H. Fischer, M. Birk, C. Blom, B. Carli, M. Carlotti, T. von Clarmann, L. Delbouille, A. Dudhia, D. Ehhalt, M. Endemann, J. M. Flaud, R. Gessner, A. Kleinert, R. Koopman, J. Langen, M. López-Puertas, P. Mosner, H. Nett, H. Oelhaf, G. Perron, J. Remedios, M. Ridolfi, G. Stiller, and R. Zander. Mipas: an instrument for atmospheric and climate research. *Atmospheric Chemistry and Physics*, 8(8):2151–2188, 2008. doi: 10.5194/acp-8-2151-2008. URL https://www.atmos-chem-phys.net/8/2151/2008/.

P. Y. Foucher, A. Chédin, R. Armante, C. Boone, C. Crevoisier, and P. Bernath. Carbon dioxide atmospheric vertical profiles retrieved from space observation using ace-fts solar occultation instrument. *Atmospheric Chemistry and Physics*, 11(6):2455–2470, 2011. doi: 10.5194/acp-11-2455-2011. URL https://www.atmos-chem-phys.net/11/2455/2011/.

Hermann Haken and Hans Christoph Wolf. *Molecular physics and elements of quantum chemistry*. Springer, 2013.

I. Morino, O. Uchino, M. Inoue, Y. Yoshida, T. Yokota, P. O. Wennberg, G. C. Toon, D. Wunch, C. M. Roehl, J. Notholt, T. Warneke, J. Messerschmidt, D. W. T. Griffith, N. M. Deutscher, V. Sherlock, B. Connor, J. Robinson, R. Sussmann, and M. Rettinger. Preliminary validation of column-averaged volume mixing ratios of carbon dioxide and methane retrieved from gosat short-wavelength infrared spectra. *Atmospheric Measurement Techniques*, 4(6):1061–1076, 2011. doi: 10.5194/amt-4-1061-2011. URL https://www.atmos-meas-tech.net/4/1061/2011/.

J. Notholt and O. Schrems. Ground-based FTIR measurements of vertical column densities of several trace gases above Spitsbergen. *Geophysical Research Letters*, 21(13):1355–1358, 1994. ISSN 1944-8007. doi: 10.1029/93GL01786. URL http://dx.doi.org/10.1029/93GL01786.

L.S. Rothman and L.D.G. Young. Infrared energy levels and intensities of carbon dioxide—II. *Journal of Quantitative Spectroscopy and Radiative Transfer*, 25(6):505 – 524, 1981. ISSN 0022-4073. doi: http://dx.doi.org/10.1016/0022-4073(81)90026-1. URL http://www.sciencedirect.com/science/article/pii/0022407381900261.

GC Toon. The jpl mkiv interferometer. *Optics and Photonics News*, 2(10):19–21, 1991.

D. Wunch, G.C. Toon, J.-F.L. Blavier, R.A. Washenfelder, J. Notholt, B.J. Connor, D.W.T. Griffith, V. Sherlock, and P.O. Wennberg. The Total Carbon Column Observing Network. *Philosophical Transactions of the Royal Society A: Mathematical, Physical and Engineering Sciences*, 369(1943): 2087–2112, 2011. doi: 10.1098/rsta.2010.0240. URL http://rsta.royalsocietypublishing.org/content/369/1943/2087.abstract.